

# Topological first-order solitons in a gauged $CP(2)$ model with the Maxwell-Chern-Simons action

R. Casana,<sup>\*</sup> N. H. Gonzalez-Gutierrez,<sup>†</sup> and E. da Hora<sup>‡</sup>

<sup>\*</sup><sup>†</sup>*Departamento de Física, Universidade Federal do Maranhão, 65080-805, São Luís, Maranhão, Brazil, and*

<sup>‡</sup>*Coordenadoria Interdisciplinar de Ciência e Tecnologia, Universidade Federal do Maranhão, 65080-805, São Luís, Maranhão, Brazil.*

We verify the existence of radially symmetric first-order solitons in a gauged  $CP(2)$  scenario in which the dynamics of the Abelian gauge field is controlled by the Maxwell-Chern-Simons action. We implement the standard Bogomol'nyi-Prasad-Sommerfield (BPS) formalism, from which we obtain a well-defined lower bound for the corresponding energy (i.e. the Bogomol'nyi bound) and the first-order equations saturating it. We solve these first-order equations numerically by means of the finite-difference scheme, therefore obtaining regular solutions of the effective model, their energy being quantized according the winding number rotulating the final configurations, as expected. We depict the numerical solutions, whilst commenting on the main properties they engender.

PACS numbers: 11.10.Kk, 11.10.Lm, 11.27.+d

## I. INTRODUCTION

Time-independent solutions of highly nonlinear equations are of great importance and interest in many areas of physics and mathematics [1]. In field theory such a highly nonlinear equations arise naturally, i.e. the second-order Euler-Lagrange equations, which can be quite hard to solve. However, under very special circumstances, genuine field solutions can be obtained via a particular set of two coupled first-order differential equations, namely the Bogomol'nyi-Prasad-Sommerfield (BPS) ones [2], the resulting configurations minimizing the energy of the overall system.

In the context of gauged (2+1)-dimensional models, these first-order solutions are called vortices. In particular, magnetic vortices were verified to occur in the Maxwell-Higgs electrodynamics [3]. Also, it was demonstrated that electrically charged vortices emerge from both the Chern-Simons-Higgs [4] and the Maxwell-Chern-Simons-Higgs scenarios [5].

Moreover, other important examples of first-order solutions include the ones arising from nonlinear sigma models (NL $\sigma$ M) [6] in the presence of a gauge field, which have been widely applied in the study of different aspects of field theory and condensed matter physics [7].

In this sense, the existence of topological solitons in a  $O(3)$  nonlinear sigma model endowed by the Maxwell action was demonstrated in [8, 9]. Moreover, in the Refs. [10, 11], the authors studied the  $O(3)$  nonlinear sigma model gauged by the Chern-Simons term, establishing the existence of both topological and nontopological configurations. The gauged  $O(3)$  sigma model with the gauge field dynamics ruled by both the Maxwell and the Chern-Simons terms was also studied [12, 13].

Topological solitons also appear in the  $CP(N-1)$  models whose importance is due to the fact that they present some fundamental properties (such as asymptotic freedom, confinement, nontrivial vacuum structure giving rise to stable instantons, etc.) typically inherent to the Yang-Mills theories [14–17].

In a recent work, the existence of first-order vortices in a gauged  $CP(2)$  model whose gauge field is ruled by the Maxwell action was proposed [18]. This hypothesis was confirmed in the Ref. [19], where the first-order formalism was implemented in a clear way, giving rise to a well-defined lower-bound for the total energy (i.e. the Bogomol'nyi bound) and to the corresponding first-order differential equations.

In the sequel, some of us have considered a gauged  $CP(2)$  scenario endowed by the Maxwell term multiplied by a nontrivial dielectric function, the resulting noncanonical model supporting nontopological first-order vortices with no quantized magnetic flux [20]. Furthermore, some of us have also calculated the topological first-order vortices inherent to a gauged  $CP(2)$  model in the presence of the Chern-Simons term (instead of the Maxwell one), see the Ref. [21].

In this context, the aim of the present manuscript is to investigate the existence of first-order solitons arising from a gauged  $CP(2)$  model in which the dynamics of the gauge sector is ruled simultaneously by both the Maxwell and the Chern-Simons terms. Therefore, in order to introduce our results, this work is organized as follows: in the next Sec. II, we define the gauged Maxwell-Chern-Simons  $CP(N-1)$  model, focusing our attention on those time-independent solitons possessing radial symmetry. We then particularize our investigation to the case  $N=3$ , from which we develop the corresponding first-order framework via the usual prescription (i.e. requiring the minimization the total energy), this way finding the resulting lower-bound for the energy itself and the first-order equations saturating it. In the Sec. III, we solve the first-order equations numerically by means of the finite-difference algorithm, from which we depict

---

\* [rodolfo.casana@gmail.com](mailto:rodolfo.casana@gmail.com)

† [neyver.hgg@gmail.com](mailto:neyver.hgg@gmail.com)

‡ [edahora.ufma@gmail.com](mailto:edahora.ufma@gmail.com)

the numerical solutions, whilst commenting on the main properties they engender. We end our work in the Section IV, in which we point out our final observations and perspectives regarding future contributions.

## II. THE OVERALL MODEL

We begin our manuscript by considering the gauged  $CP(N-1)$  model [18] in the presence of the usual Chern-Simons term, the corresponding Lagrange density standing for

$$\mathcal{L}_0 = \mathcal{L}_{MCS} + (P_{ab}D_\mu\phi_b)^* P_{ac}D^\mu\phi_c - U(|\phi|), \quad (1)$$

where

$$\mathcal{L}_{MCS} = \mathcal{L}_M + \mathcal{L}_{CS}, \quad (2)$$

with

$$\mathcal{L}_M = -\frac{1}{4}F_{\mu\nu}F^{\mu\nu} \quad \text{and} \quad \mathcal{L}_{CS} = -\frac{\kappa}{4}\epsilon^{\rho\mu\nu}A_\rho F_{\mu\nu}. \quad (3)$$

Here,  $F_{\mu\nu} = \partial_\mu A_\nu - \partial_\nu A_\mu$  is the standard electromagnetic field strength tensor and  $D_\mu\phi_a = \partial_\mu\phi_a - igA_\mu Q_{ab}\phi_b$  stands for the corresponding covariant derivative. Also,  $P_{ab} = \delta_{ab} - h^{-1}\phi_a\phi_b^*$  is a projection operator introduced for the sake of convenience, whilst  $Q_{ab}$  represents a real and diagonal charge matrix. In the present case, the  $CP(N-1)$  field is assumed to satisfy  $\phi_a^*\phi_a = h$ .

The corresponding Euler-Lagrange equations for the gauge and scalar sectors are, respectively,

$$\partial_\mu F^{\mu\rho} - \frac{\kappa}{2}\epsilon^{\rho\mu\nu}F_{\mu\nu} = J^\rho \quad (4)$$

and

$$2P_{ad}D_\mu(P_{dc}D^\mu\phi_c) - P_{ad}D_\mu D^\mu\phi_d = -P_{ad}\frac{\partial U}{\partial\phi_d^*}, \quad (5)$$

where

$$J^\mu = ig[(P_{ab}D^\mu\phi_b)^*(P_{ac}Q_{cd}\phi_d) - \text{h.c.}] \quad (6)$$

stands for the current 4-vector (conserved). Here, h.c. means Hermitian conjugate.

We look for the time-independent solutions arising from (1). In this sense, it is instructive to write down the Gauss law for static configurations, i.e., (here,  $B = F_{12}$  is the magnetic field)

$$\partial_j\partial_j A_0 + \kappa B = 2g^2 A^0 (P_{ac}Q_{cd}\phi_d)^* P_{ab}Q_{bm}\phi_m, \quad (7)$$

the corresponding solutions possessing both magnetic and electric fields.

In addition, the time-independent Ampère's law can be written as

$$\partial_k B + \kappa\partial_k A_0 = -\epsilon_{kj}J_j, \quad (8)$$

with

$$J_k = ig[(P_{ab}D_k\phi_b)^*(P_{ac}Q_{cd}\phi_d) - \text{h.c.}], \quad (9)$$

the equation of motion for the static scalar sector reading

$$\begin{aligned} & 2P_{ad}D_k(P_{dc}D_k\phi_c) - P_{ad}D_k D_k\phi_d \\ & - P_{ad}\frac{\partial U}{\partial\phi_d^*} + 2g^2(A_0)^2 P_{ad}Q_{db}P_{bc}Q_{ce}\phi_e \\ & - g^2(A_0)^2 P_{ad}Q_{db}Q_{be}\phi_e = 0. \end{aligned} \quad (10)$$

It can be shown that the Lagrange density (1) does not support solitonic configurations satisfying a well-defined first-order framework. However, the existence of planar first-order solitons carrying both magnetic and electric fields becomes possible via the introduction of a neutral scalar field  $\Psi$  into the Lagrange density (1), the resulting model being described by

$$\begin{aligned} \mathcal{L} = & \mathcal{L}_{MCS} + (P_{ab}D_\mu\phi_b)^* P_{ac}D^\mu\phi_c + \frac{1}{2}\partial_\mu\Psi\partial^\mu\Psi \\ & - g^2\Psi^2(P_{ab}Q_{bd}\phi_d)^* P_{ac}Q_{ce}\phi_e - U(|\phi|, \Psi), \end{aligned} \quad (11)$$

$U(|\phi|, \Psi)$  standing for the potential describing the scalar-matter self-interaction (to be determined later).

Here, it is worthwhile to point out that the introduction of such a neutral field is a well-established prescription supporting the consistent study of first-order configurations in the presence of the Chern-Simons term. This prescription was firstly used in the context of the Maxwell-Chern-Simons-Higgs theories [22, 23], the main motivation coming from supersymmetric arguments. It was also implemented successfully in connection to non-linear sigma models [12, 13], being also used to describe charged solitons arising from Lorentz-violating scenarios [24–27].

Along of the remain of this manuscript, we consider the  $N = 3$  case, this way reducing our study to the  $CP(2)$  scenario. We then focus our attention on those time-independent solutions presenting radial symmetry which are implemented via the standard *Ansatz*

$$A_0 = A_0(r) \quad \text{and} \quad A_i = -\frac{1}{gr^2}\epsilon_{ij}x_j A(r), \quad (12)$$

$$\begin{pmatrix} \phi_1 \\ \phi_2 \\ \phi_3 \end{pmatrix} = h^{1/2} \begin{pmatrix} e^{in_1\theta} \sin\alpha(r) \cos\beta(r) \\ e^{in_2\theta} \sin\alpha(r) \sin\beta(r) \\ e^{in_3\theta} \cos\alpha(r) \end{pmatrix}, \quad (13)$$

where  $\epsilon_{ij}$  stands for the bidimensional Levi-Civita tensor (with  $\epsilon_{12} = +1$ ),  $x_i = r(\cos\theta, \sin\theta)$  is the position vector (written in polar coordinates) and the integers  $n_1$ ,  $n_2$  and  $n_3$  represent the winding numbers (vorticities) of the corresponding scalar solutions.

Now, it is important to highlight that, concerning the combination between the charge matrix  $Q_{ab}$  and the winding numbers  $n_1$ ,  $n_2$  and  $n_3$ , there are two possible choices supporting the existence of topological solitons:

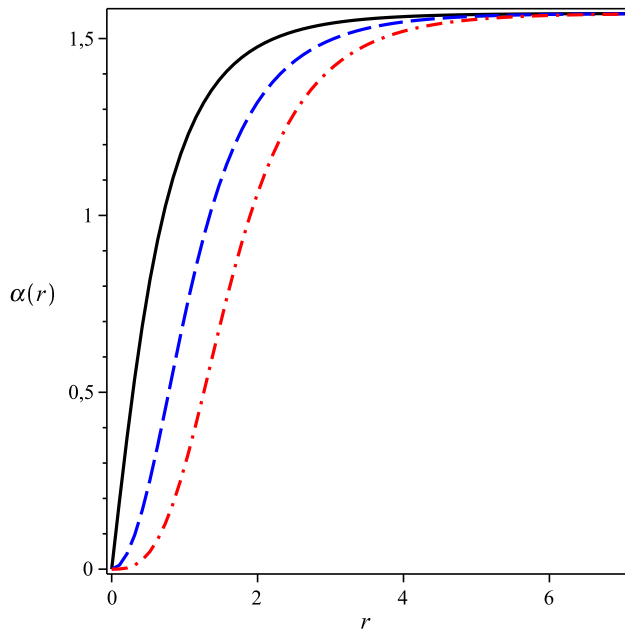


FIG. 1. Numerical solutions to the profile function  $\alpha(r)$  for  $n = 1$  (solid black line),  $n = 2$  (dashed blue line) and  $n = 3$  (dotted red line). Here,  $h = \kappa = 1$  and  $g = 2$ .

(i)  $Q = \lambda_3/2$  and  $n_1 = -n_2 = n$ , and (ii)  $Q = \lambda_8/2$  and  $n_1 = n_2 = n$  (both ones with  $n_3 = 0$ ,  $\lambda_3$  and  $\lambda_8$  being the diagonal Gell-Mann matrices, i.e.,  $\lambda_3 = \text{diag}(1, -1, 0)$  and  $\sqrt{3}\lambda_8 = \text{diag}(1, 1, -2)$ ). Nevertheless, in [18], the author have demonstrated that these two combinations simply mimic each other, this way existing only one effective scenario. Therefore, in this manuscript, we investigate only the case defined by  $n_1 = -n_2 = n$ ,  $n_3 = 0$  and

$$Q_{ab} = \frac{1}{2}\lambda_3 = \frac{1}{2}\text{diag}(1, -1, 0). \quad (14)$$

Furthermore, given the Ansatz (12) and (13) and the conventions stated above, one gets that nonsingular solutions possessing finite-energy are attained by those profile functions  $\alpha(r)$ ,  $A(r)$  and  $A_0(r)$  obeying the boundary conditions

$$\alpha(r=0) = 0, \quad A(r=0) = 0, \quad A'_0(r=0) = 0, \quad (15)$$

and

$$\alpha(r \rightarrow \infty) \rightarrow \frac{\pi}{2}, \quad A(r \rightarrow \infty) \rightarrow 2n, \quad A_0(r \rightarrow \infty) \rightarrow 0, \quad (16)$$

where prime denotes the derivative with respect to the radial coordinate  $r$ . Here, it is important to point out that the boundary conditions for  $\alpha(r)$  and  $A(r)$  are well-established in the literature [18]. In addition, we verify the conditions for the electric potential  $A_0(r)$  in the Sec. III below.

It is also instructive to write down the equation of motion for the additional profile function  $\beta(r)$ , i.e. (here,

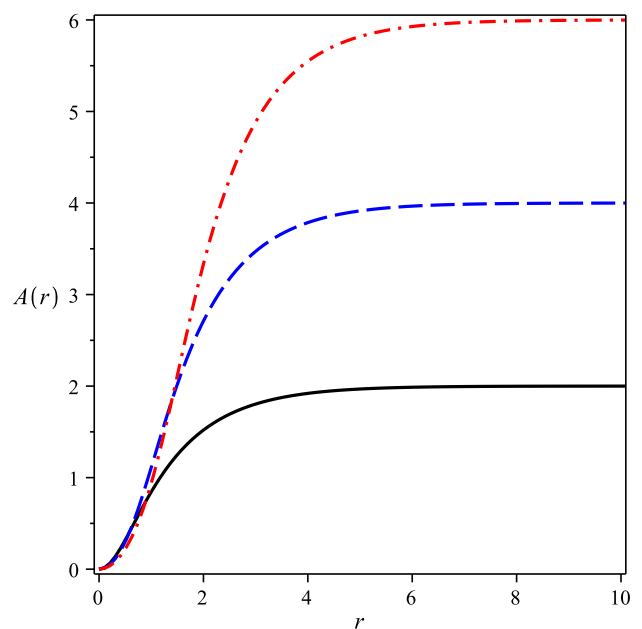


FIG. 2. Numerical solutions to the profile function  $A(r)$ . Conventions as in the Fig. 1. The solutions reach the asymptotic value  $A(r \rightarrow \infty) \rightarrow 2n$  in a monotonic way, as expected.

we have defined  $H_{\pm}(r) = (A_0)^2 \pm \Psi^2$ , for the sake of simplicity)

$$\begin{aligned} \frac{d^2\beta}{dr^2} + \left(\frac{1}{r} + 2\cot\alpha\frac{d\alpha}{dr}\right)\frac{d\beta}{dr} + \frac{g^2}{4}H_-(r)\sin^4\alpha\sin(4\beta) \\ - \frac{\sin^2\alpha\sin(4\beta)}{r^2}\left(n - \frac{A}{2}\right)^2 = 0, \end{aligned} \quad (17)$$

whose two possible solutions are

$$\beta_1 = \frac{\pi}{4} + \frac{\pi}{2}k \quad \text{or} \quad \beta_2 = \frac{\pi}{2}k, \quad (18)$$

with  $k \in \mathbb{Z}$ . These solutions define *a priori* two different scenarios. However, the expressions arising from  $\beta(r) = \beta_2$  can be obtained directly from those inherent to  $\beta(r) = \beta_1$  via the transformations  $\alpha \rightarrow \alpha/2$  and  $h \rightarrow 4h$ . Hence, we conclude that these two a priori different solutions are phenomenologically equivalent, this way existing only one effective scenario. So, in what follows, we only consider the case  $\beta(r) = \beta_1$ .

We now look for first-order differential equations supporting radially symmetric solutions of the model (11). As it is usual, we proceed the minimization of the corresponding energy, the starting-point being the energy-momentum tensor inherent to (11), i.e.,

$$\begin{aligned} \mathcal{T}_{\rho\sigma} = -F_{\rho\mu}F_{\sigma}^{\mu} + \partial_{\rho}\Psi\partial_{\sigma}\Psi + (P_{ab}D_{\rho}\phi_b)^*P_{ac}D_{\sigma}\phi_c \\ + (P_{ab}D_{\sigma}\phi_b)^*P_{ac}D_{\rho}\phi_c - g_{\rho\sigma}\mathcal{L}_N, \end{aligned} \quad (19)$$

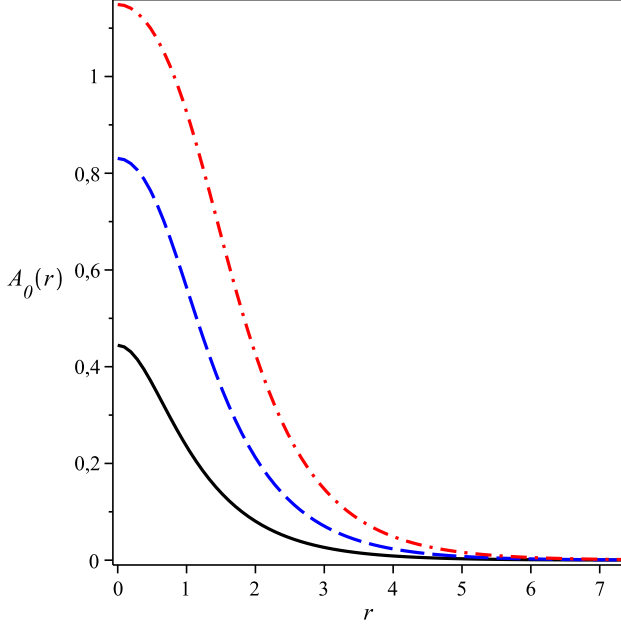


FIG. 3. Numerical solutions to the gauge function  $A_0(r)$ . Conventions as in the Fig. 1,  $A_0(0) \equiv A_0(r=0)$  increasing with the vorticity.

where

$$\begin{aligned} \mathcal{L}_N = \mathcal{L}_M + (P_{ab}D_\mu\phi_b)^* P_{ac}D^\mu\phi_c + \frac{1}{2}\partial_\mu\Psi\partial^\mu\Psi \\ - g^2\Psi^2 (P_{ab}Q_{bd}\phi_d)^* P_{ac}Q_{ce}\phi_e - U \end{aligned} \quad (20)$$

stands for the nontopological part of the Lagrange density (11). Thus, one gets the radially symmetric energy density to be

$$\begin{aligned} \varepsilon = \frac{1}{2}B^2 + U + \frac{1}{2}\left(\frac{dA_0}{dr}\right)^2 + \frac{1}{2}\left(\frac{d\Psi}{dr}\right)^2 \\ + h\left[\left(\frac{d\alpha}{dr}\right)^2 + \frac{W}{4r^2}(2n-A)^2\sin^2\alpha\right] \\ + h\left[\left(\frac{d\beta}{dr}\right)^2 + \frac{g^2W}{4}H_+(r)\right]\sin^2\alpha, \end{aligned} \quad (21)$$

where we have introduced the auxiliary function

$$W(\alpha, \beta) = 1 - \sin^2\alpha \cos^2(2\beta), \quad (22)$$

the magnetic field  $B(r)$  being given by

$$B(r) = \frac{1}{gr} \frac{dA}{dr}, \quad (23)$$

according the *Ansatz* (12) and (13). Here,  $U = U(\alpha, \Psi)$  represents self-interacting potential.

We now choose the particular solution

$$\beta(r) = \beta_1 = \frac{\pi}{4} + \frac{\pi}{2}k, \quad (24)$$

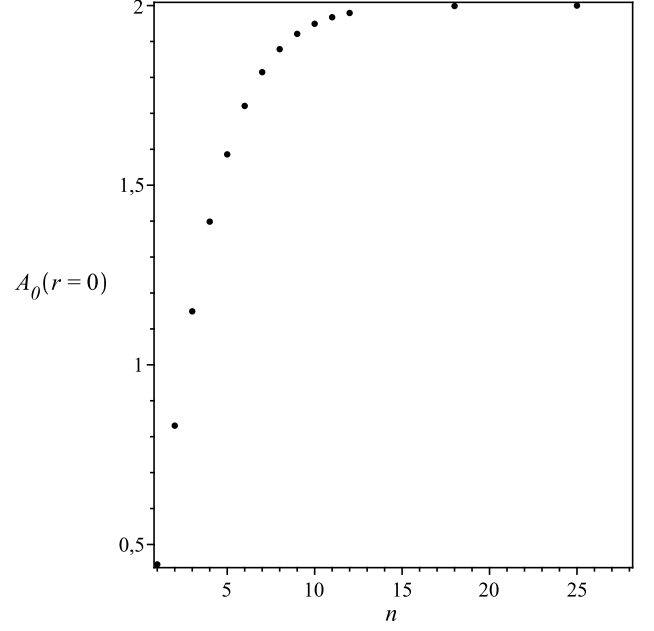


FIG. 4. The dependence of  $A_0(0) \equiv A_0(r=0)$  with the vorticity: given  $h = \kappa = 1$  and  $g = 2$ , the scalar potential reaches  $A_0^{\max}(r=0) = 2$  for sufficiently large values of  $n$ .

from which we get  $W(\alpha, \beta = \beta_1) = 1$ , the energy density (21) being reduced to

$$\begin{aligned} \varepsilon = \frac{1}{2}B^2 + U + h\left(\frac{d\alpha}{dr}\right)^2 + \frac{h}{4r^2}(2n-A)^2\sin^2\alpha \\ + \frac{1}{2}\left(\frac{dA_0}{dr}\right)^2 + \frac{1}{2}\left(\frac{d\Psi}{dr}\right)^2 + \frac{g^2h}{4}H_+\sin^2\alpha, \end{aligned} \quad (25)$$

which can be rewritten as

$$\begin{aligned} \varepsilon = \frac{1}{2}\left(B \mp \sqrt{2U}\right)^2 + h\left[\frac{d\alpha}{dr} \mp \frac{(2n-A)}{2r}\sin\alpha\right]^2 \\ + \frac{1}{2}\left(\frac{d\Psi}{dr} \pm \frac{dA_0}{dr}\right)^2 + \frac{g^2h}{4}(\Psi \pm A_0)^2\sin^2\alpha \\ \pm B\sqrt{2U} \pm h\frac{(2n-A)}{r}\frac{d\alpha}{dr}\sin\alpha \\ \mp \frac{d\Psi}{dr}\frac{dA_0}{dr} \mp \frac{g^2h}{2}\Psi A_0\sin^2\alpha. \end{aligned} \quad (26)$$

Here, it is useful to note that, in view of (12) and (13), the time-independent Gauss law (7) can be written in the form (note that such equation remains the same after the introduction of the neutral scalar field  $\Psi$ ),

$$\frac{d^2A_0}{dr^2} + \frac{1}{r}\frac{dA_0}{dr} + \kappa B = \frac{g^2h}{2}A_0\sin^2\alpha. \quad (27)$$

It allows the last term in (26) can be rewritten as

$$\frac{g^2h}{2}A_0\Psi\sin^2\alpha = \Psi\frac{d^2A_0}{dr^2} + \frac{\Psi}{r}\frac{dA_0}{dr} + \kappa\Psi B, \quad (28)$$

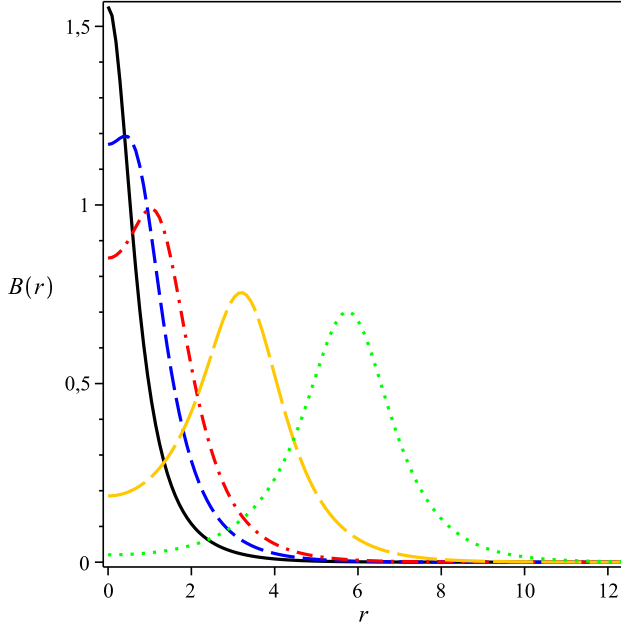


FIG. 5. Numerical solutions to the magnetic field  $B(r)$ . Conventions as in the Fig. 1, the long-dashed orange line (dotted green line) representing the solution for  $n = 7$  ( $n = 12$ ).

consequently, the energy density (26) being reduced to be

$$\begin{aligned} \varepsilon = & \frac{1}{2} \left( B \mp \sqrt{2U} \right)^2 + h \left[ \frac{d\alpha}{dr} \mp \frac{(2n-A)}{2r} \sin \alpha \right]^2 \\ & + \frac{1}{2} \left( \frac{d\Psi}{dr} \pm \frac{dA_0}{dr} \right)^2 + \frac{1}{4} h g^2 (\Psi \pm A_0)^2 \sin^2 \alpha \\ & \pm B \left( \sqrt{2U} - h g \cos \alpha - \kappa \Psi \right) \\ & \mp \frac{h}{r} \frac{d}{dr} [(2n-A) \cos \alpha] \mp \frac{1}{r} \frac{d}{dr} \left( r \Psi \frac{dA_0}{dr} \right). \end{aligned} \quad (29)$$

Due to the boundary conditions, the last term in (29) (i.e. the total derivative  $r^{-1} (r \Psi A_0')'$ ) gives null contribution to the total energy, so we neglect it. However, the penultimate total derivative provides a nonvanishing contribution to the overall energy.

The potential  $U(|\phi|, \Psi)$  is determined by choosing

$$U(\alpha, \Psi) = \frac{1}{2} (h g \cos \alpha + \kappa \Psi)^2, \quad (30)$$

so, the resulting total energy being given by

$$\begin{aligned} E = & \pm 4\pi h n + 2\pi \int_0^\infty r \left\{ \frac{1}{2} \left[ B \mp (h g \cos \alpha + \kappa \Psi) \right]^2 \right. \\ & + \frac{1}{2} \left( \frac{d\Psi}{dr} \pm \frac{dA_0}{dr} \right)^2 + \frac{g^2 h}{4} (\Psi \pm A_0)^2 \sin^2 \alpha \\ & \left. + h \left[ \frac{d\alpha}{dr} \mp \frac{(2n-A)}{2r} \sin \alpha \right]^2 \right\} dr. \end{aligned} \quad (31)$$

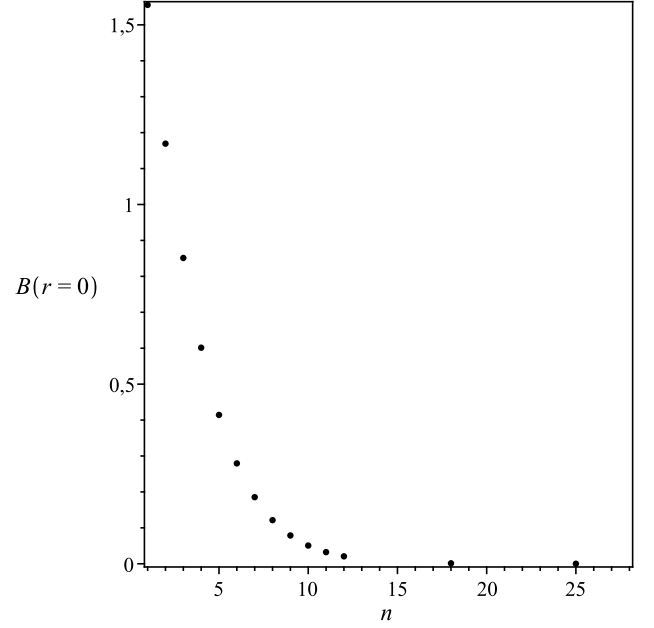


FIG. 6. The dependence of  $B(0)$  with the vorticity: the difference  $b_0 = gh - \kappa A_0(0)$  vanishes for sufficiently large values of  $n$ .

The expression in (31) reveals that the energy of the effective model supports a well-defined lower-bound given by

$$E_{bps} = \pm 4\pi h n = \mp 2\pi \int_0^\infty dr r \frac{h}{r} \frac{d}{dr} [(2n-A) \cos \alpha], \quad (32)$$

which is attained by those fields satisfying the set of differential equations

$$\frac{d\alpha}{dr} = \pm \frac{(2n-A)}{2r} \sin \alpha, \quad (33)$$

$$B = \pm (h g \cos \alpha + \kappa \Psi), \quad (34)$$

$$\frac{d\Psi}{dr} = \mp \frac{dA_0}{dr} \quad \text{and} \quad \Psi = \mp A_0, \quad (35)$$

which therefore stand for the first-order equations inherent to the effective radially symmetric model.

Here, it is interesting to highlight that the last two equations are automatically satisfied by  $\Psi = \mp A_0$ , the resulting configurations being then obtained via the two remaining first-order equations, i.e.

$$\frac{d\alpha}{dr} = \pm \frac{(2n-A)}{2r} \sin \alpha, \quad (36)$$

$$B = \frac{1}{gr} \frac{dA}{dr} = \pm h g \cos \alpha - \kappa A_0, \quad (37)$$

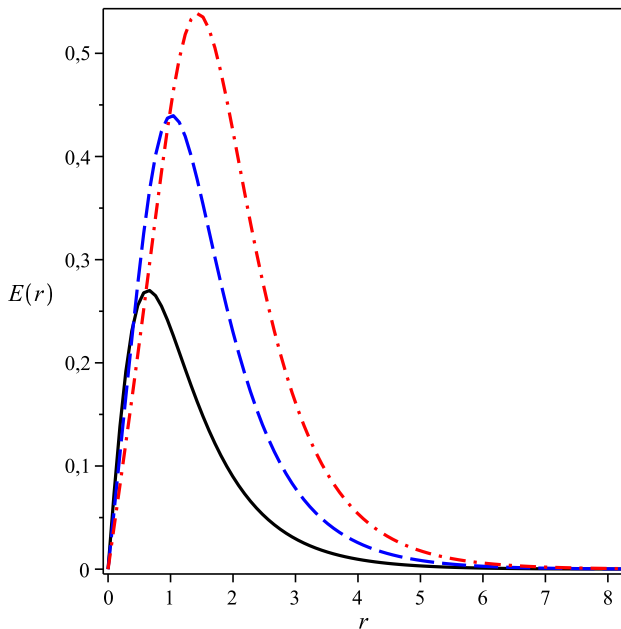


FIG. 7. Numerical solutions to the electric field  $E(r)$ . Conventions as in the Fig. 1,  $E(r=0)$  and  $E(r \rightarrow \infty)$  vanishing.

which must be solved together with the Gauss law (27),

$$\frac{d^2 A_0}{dr^2} + \frac{1}{r} \frac{dA_0}{dr} + \kappa B = \frac{g^2 h}{2} A_0 \sin^2 \alpha. \quad (38)$$

In addition, the reader can verify that the solutions for  $n < 0$  (anti-vortices) can be obtained directly from the ones for  $n > 0$  (vortices) via the transformations  $n \rightarrow -n$ ,  $\alpha \rightarrow \alpha$ ,  $A \rightarrow -A$  and  $A_0 \rightarrow -A_0$ .

Moreover, another quantity commonly referred when studying vortices is the magnetic flux  $\Phi_B$  they give rise. In the present case, the resulting flux reads

$$\Phi_B = 2\pi \int_0^\infty r B(r) dr = \frac{4\pi}{g} n. \quad (39)$$

In this case, whether we consider

$$\rho(r) = \frac{g^2 h}{2} A_0 \sin^2 \alpha \quad (40)$$

as the electric charge density, the magnetic flux  $\Phi_B$  (39) can be verified to be proportional to the total electric charge  $\mathcal{Q}$ , i.e.

$$\mathcal{Q} = 2\pi \int_0^\infty r \rho(r) dr = \kappa \Phi_B, \quad (41)$$

where we have integrated the Gauss law (27).

### III. FIRST-ORDER SOLUTIONS

We now proceed the analysis of the differential equations (36), (37), (38) themselves in view of the boundary

conditions (15) and (16). It is useful to check *a priori* whether the solutions attain the boundary values (15) and (16) correctly. In order to verify such a convergence, we proceed to solve the differential equations (36), (37) and (38) around those values. By considering  $n > 0$ , we calculate the approximate solutions near the origin to be

$$\alpha(r) \approx C_n r^n, \quad (42)$$

$$A(r) \approx \frac{g}{2} (gh - \kappa A_0(0)) r^2,$$

$$A_0(r) \approx A_0(0) - \frac{\kappa}{4} (gh - \kappa A_0(0)) r^2, \quad (43)$$

where  $C_n$  and  $A_0(0) \equiv A_0(r=0)$  are positive constants to be determined numerically for each value of the vorticity  $n$ , the last solution verifying the boundary value for  $A_0(r=0)$  appearing in (15).

A similar procedure reveals that the asymptotic profiles are (here, the positive constant  $C_\infty$  also depends on  $n$ )

$$\alpha(r) \approx \frac{\pi}{2} - C_\infty e^{-M_\alpha r}, \quad (44)$$

$$A(r) \approx 2n - 2MC_\infty r e^{-M_A r},$$

$$A_0(r) \approx \frac{2M}{g} C_\infty e^{-M r}, \quad (45)$$

where the parameters

$$M_\alpha = M_A = M = \frac{1}{2} \left( \sqrt{2g^2 h + \kappa^2} - |\kappa| \right) \quad (46)$$

represent the masses of the corresponding bosons (the relation  $M_\alpha/M_A = 1$  defining the BPS point). In this case, it is easy to verify that, in the limit  $g \gg \kappa$ , the masses behave like those arising from a gauged  $CP(2)$  theory endowed by the Maxwell term only [18],

$$M \approx g \sqrt{\frac{h}{2}}. \quad (47)$$

On the other hand, when  $g \ll \kappa$ , the masses mimic the value obtained from a gauged  $CP(2)$  model in the presence of the Chern-Simons action alone [21]:

$$M \approx \frac{g^2 h}{2\kappa}. \quad (48)$$

In what follows, we proceed the numerical integration of the equations (36), (37), (38) according the conditions (15) and (16). We solve the corresponding system by means of finite-difference algorithm, from which we depict the resulting profiles in the figures 1, 2, 3, 4, 5 and 6. Here, we choose  $h = \kappa = 1$  and  $g = 2$ , plotting the solutions for  $n = 1$  (solid black line),  $n = 2$  (dashed blue line) and  $n = 3$  (dotted red line).

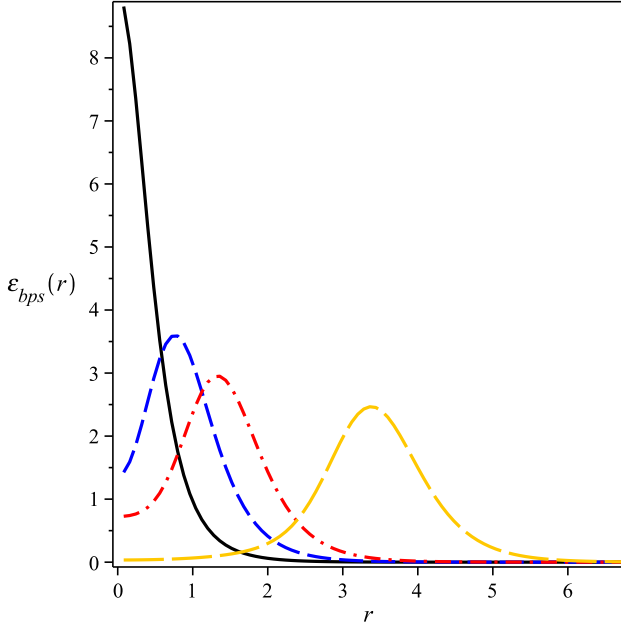


FIG. 8. Numerical solutions to the energy distribution  $\varepsilon_{bps}(r)$ . Conventions as in the Fig. 5, the resulting structures being similar to the magnetic ones.

The figures 1 and 2 show the numerical solutions to the profile functions  $\alpha(r)$  and  $A(r)$ , respectively, from which we see that these two solutions reach the boundary values in a monotonic way, as expected. In particular, the gauge function obeys  $A(r \rightarrow \infty) \rightarrow 2n$ .

In the Figure 3, we depict the numerical profile of the scalar potential  $A_0(r)$ , the corresponding structures being lumps centered at  $r = 0$ . It is interesting to note how  $A_0(0) \equiv A_0(r = 0)$  depends on  $n$ , its value increasing as the vorticity itself increases until reaching the maximum value

$$A_0^{max}(r = 0) = \frac{gh}{\kappa}, \quad (49)$$

for sufficiently large values of  $n$  (see the Figure 4).

The Figure 5 presents the solutions for the magnetic field  $B(r)$ , including the ones obtained for  $n = 7$  (long-dashed orange line) and  $n = 12$  (dotted green line). In this case, for  $n = 1$ , the profile is a well-defined lump centered at the origin. On the other hand, for  $n > 1$ , the solutions stand for rings also centered at  $r = 0$ , their amplitudes (radii) decreasing (increasing) as the vorticity increases.

It is particularly interesting to consider the solution for  $B(r)$  coming from (42). It reads

$$B(r) \approx b_0 + \frac{1}{4} \left( \kappa^2 b_0 - 2(C_1)^2 gh \right) r^2, \quad (50)$$

for  $n = 1$ , and

$$B(r) \approx b_0 + \frac{\kappa^2 b_0}{4} r^2, \quad (51)$$

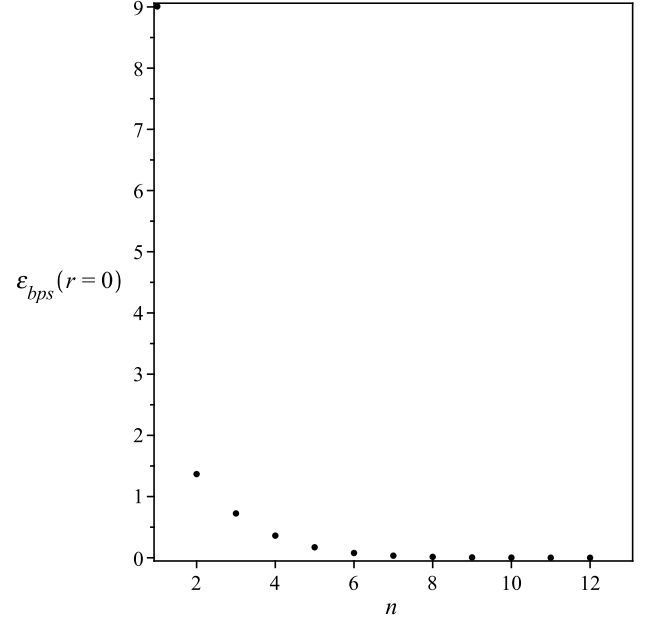


FIG. 9. The dependence of  $\varepsilon_{bps}(0)$  with the vorticity: for  $n = 1$ , one gets  $\varepsilon_{bps}(r = 0) = 2(C_1)^2 h + b_0^2$ .

for  $n \geq 2$ , where we have defined

$$b_0 = gh - \kappa A_0(0). \quad (52)$$

In this sense, we get that value of  $B(r = 0)$ , i.e.

$$B(r = 0) = b_0 = gh - \kappa A_0(0), \quad (53)$$

which explains the behavior of the magnetic field at the origin: as  $n$  increases, the value of  $A_0(r = 0)$  increases too (see the Figure 4), whilst the difference  $b_0 = gh - \kappa A_0(0)$  decreases, see the Figure 6. In particular, for sufficiently large values of the vorticity, one gets that  $A_0(r = 0) \rightarrow gh/\kappa$  and  $B(r = 0) = b_0 \rightarrow 0$ .

The solutions to the electric field  $E(r)$  appear in the Figure 7, from which we see that the resulting configurations are rings centered at  $r = 0$ , their amplitude and radii increasing as the vorticity increases, with both  $E(r = 0)$  and  $E(r \rightarrow \infty)$  vanishing.

We depict the numerical profiles to the energy distribution  $\varepsilon_{bps}(r)$  in the Figure 8, from which see that the resulting structures are similar to the magnetic ones, i.e. for  $n = 1$  ( $n > 1$ ) the solution is a lump (ring) centered at  $r = 0$ . Thus, it is instructive to study the behavior of  $\varepsilon_{bps}(r)$  near the origin which results to be

$$\varepsilon_{bps}(r) \approx 2(C_1)^2 h + (b_0)^2 + \varepsilon_2 r^2, \quad (54)$$

from  $n = 1$ , and

$$\varepsilon_{bps}(r) \approx (b_0)^2 + \frac{3}{4} (b_0 \kappa)^2 r^2, \quad (55)$$

for  $n \geq 2$ . Here, we have defined

$$\varepsilon_2 = \frac{3}{4} (b_0 \kappa)^2 - \frac{2}{3} (C_1)^4 h + \frac{gh}{2} (C_1)^2 \left[ (A_0(0))^2 g - 4b_0 \right], \quad (56)$$

for the sake of convenience.

We therefore note that, as  $n$  increases,  $\varepsilon_{bps}(r = 0)$  vanishes. In particular, for  $n = 1$ , one gets that  $\varepsilon_{bps}(r = 0) = 2(C_1)^2 h + (b_0)^2$ , see the Figure 9.

#### IV. FINAL COMMENTS AND PERSPECTIVES

We have shown the existence of radially symmetric first-order solitons in a gauged  $CP(2)$  model endowed by the Maxwell and the Chern-Simons terms simultaneously.

The point to be raised here is that, in order to implement the Bogomol'nyi prescription correctly, we have introduced a neutral scalar field into the original Maxwell-Chern-Simons model (1), such a modification being a well-known procedure usually performed when the dynamics of the gauge sector is controlled by the composite Maxwell-Chern-Simons action. Such a procedure also works in the Lorentz-violating extensions of the simplest Maxwell-Chern-Simons-Higgs theory and of the  $O(3)$ -sigma model with the Maxwell-Chern-Simons term [24–27].

We also have calculated the self-interacting potential engendering self-duality, from which we also have determined the lower-bound for the overall energy (i.e. the Bogomol'nyi bound) and the corresponding first-order differential equations supporting topological soli-

tons. Moreover, we have verified that the resulting Bogomol'nyi bound is proportional to the topological charge of the model, both ones being quantized according the vorticity  $n$ , as expected. In addition, we have rewritten the total electric charge  $\mathcal{Q}$  in terms of the magnetic flux  $\Phi_B$ , which is also quantized, see the equations (39) and (41).

We are now studying the existence of nontopological solitons in a gauged  $CP(2)$  scenario in the presence of the Chern-Simons and of the Maxwell-Chern-Simons terms, from which we hope interesting results to be reported in a future contribution.

#### ACKNOWLEDGMENTS

This work was supported by the Brazilian Government via the Conselho Nacional de Desenvolvimento Científico e Tecnológico (CNPq), the Coordenação de Aperfeiçoamento de Pessoal de Nível Superior (CAPES), and the Fundação de Amparo à Pesquisa e ao Desenvolvimento Científico e Tecnológico do Maranhão (FAPEMA). In particular, RC thanks the support from the grants CNPq/306385/2015-5, FAPEMA/Universal-00782/15 and FAPEMA/Universal-01131/17, NHGG acknowledges the full support from CAPES (postgraduate scholarship), and EH thanks the support from the grants CNPq/307545/2016-4 and CNPq/449855/2014-7.

- 
- [1] N. Manton and P. Sutcliffe, *Topological Solitons* (Cambridge University Press, Cambridge, 2004).
  - [2] E. B. Bogomol'nyi, Sov. J. Nucl. Phys. **24**, 449 (1976) [*Yad. Fiz.* **24**, 861 (1976)]. M. Prasad and C. Sommerfield, Phys. Rev. Lett. **35**, 760 (1975).
  - [3] H. B. Nielsen and P. Olesen, Nucl. Phys. B **61**, 45 (1973).
  - [4] R. Jackiw and E. J. Weinberg, Phys. Rev. Lett. **64**, 2234 (1990). R. Jackiw, K. Lee and E. J. Weinberg, Phys. Rev. D **42**, 3488 (1990).
  - [5] C. Lee, K. Lee and H. Min, Phys. Lett. B **252**, 79 (1990).
  - [6] A. A. Belavin and A. M. Polyakov, JETP Lett. **22**, 245 (1975).
  - [7] R. Rajaraman, *Solitons and Instantons* (North-Holland, Amsterdam, 1982). W. J. Zakrzewski, *Low Dimensional Sigma Models* (Hilger, Bristol, 1989).
  - [8] B. J. Schroers, Phys. Lett. B **356**, 291 (1995).
  - [9] P. Mukherjee, Phys. Rev. D **58**, 105025 (1998).
  - [10] P. K. Ghosh and S. K. Ghosh, Phys. Lett. B **366**, 199 (1996).
  - [11] P. Mukherjee, Phys. Lett. B **403**, 70 (1997).
  - [12] K. Kimm, K. Lee and T. Lee, Phys. Rev. D **53**, 4436 (1996).
  - [13] J. Han, H.-S. Nam, Lett. Math. Phys. **73**, 17 (2005).
  - [14] A. D'Adda, M. Luscher and P. D. Vecchia, Nucl. Phys. B **146**, 63 (1978).
  - [15] E. Witten, Nucl. Phys. B **149**, 285 (1979).
  - [16] A. M. Polyakov, Phys. Lett. B **59**, 79 (1975).
  - [17] M. Shifman and A. Yung, Rev. Mod. Phys. **79**, 1139 (2007).
  - [18] A. Yu. Loginov, Phys. Rev. D **93**, 065009 (2016).
  - [19] R. Casana, M. L. Dias and E. da Hora, Phys. Lett. B **768**, 254 (2017).
  - [20] R. Casana, M. L. Dias and E. da Hora, Phys. Rev. D. **96**, 076013 (2017).
  - [21] V. Almeida, R. Casana and E. da Hora, Phys. Rev. D **97**, 016013 (2018).
  - [22] C. K. Lee, K. M. Lee and H. Min, Phys. Lett. B **252**, 79 (1990).
  - [23] S. Bolognesi and S. B. Gudnason, Nucl. Phys. B **805**, 104 (2008).
  - [24] R. Casana, M. M. Ferreira, Jr., E. da Hora and C. Miller, Phys. Lett. B **718**, 620 (2012).
  - [25] R. Casana and G. Lazar, Phys. Rev. D **90**, 065007 (2014).
  - [26] R. Casana, C. F. Farias and M. M. Ferreira Jr., Phys. Rev. D **92**, 125024 (2015).
  - [27] R. Casana, C. F. Farias, M. M. Ferreira Jr. and G. Lazar, Phys. Rev. D **94**, 065036 (2016).